DIAL WITH HETERODYNE DETECTION INCLUDING SPECKLE NOISE: AIRCRAFT/SHUTTLE MEASUREMENTS OF O_3, H_2O, AND NH_3 WITH PULSED TUNABLE CO_2 LASERS

Philip Brockman, Robert V. Hess, Leo D. Staton, and Clayton H. Bair
Langley Research Center

INTRODUCTION

There is great need for atmospheric trace constituent measurements with higher vertical resolution than attainable with passive radiometers. Infrared (IR) DIAL, which depends on Mie scattering from aerosols, has special advantages for tropospheric and lower stratospheric applications and has great potential importance for measurements from Shuttle (ref. 1) and aircraft. Differential-absorption LIDAR data reduction involves comparing large amplitude signals which have small differences. The accuracy of the trace constituent concentration inferred from DIAL measurements depends strongly on the errors in determining the amplitude of the signals. Thus, the commonly used SNR expression (signal divided by noise in the absence of signal) is not adequate to describe DIAL measurement accuracy and must be replaced by an expression which includes the random coherent (speckle) noise within the signal (refs. 2, 3, and 4). A comprehensive DIAL computer algorithm (ref. 5) is modified to include heterodyne detection and speckle noise. Results of a parametric study are presented and comparisons with direct detection are discussed. Examples are given for monitoring vertical distributions of O_3, H_2O, and NH_3 using a ground-, aircraft-, or Shuttle-based pulsed tunable CO_2 laser DIAL system.

ANALYSIS OF DIAL SENSITIVITY WITH HETERODYNE DETECTION

The expectation value P of the number of measured photons from one coherence area of a scattering cell at range R of length Δr is

$$P = \frac{\eta\Gamma E\Delta r A\beta}{h\nu R^2} \exp \int_o^R -2(\xi + \sigma\rho)dr \qquad (1)$$

where η = detector efficiency, Γ = optical efficiency, E = laser energy, β = 180° backscatter coefficient per length per steradian, Δr = cell length = $\frac{cT}{2}$, T = integration time, ν = frequency, A = transmitter area (= receiver area for heterodyne system with single detector), ξ = extinction coefficient (total minus that of measured gas), σ = absorption coefficient of measured gas, and ρ = density of gas being measured.

In differential absorption, measurements are made of two frequencies selected to maximize signal and differential absorption of the species being measured while minimizing interference effects. The double ratio of signals at

adjacent scattering cells at two frequencies yields information about absorption in the region between the scattering cells.

$$\int_{R_1}^{R_2}(\rho\Delta\sigma)dr = \ln\left(\frac{P_{22}\,P_{11}}{P_{12}\,P_{21}}\right) + \ln\left(\frac{\beta_{12}\,\beta_{21}}{\beta_{11}\,\beta_{22}}\right) - 2\int_{R_1}^{R_2}(\Delta\xi)\,dr \qquad (2)$$

where P_{ij} = expectation value of measured return from cell j at frequency i. β_{ij} = backscatter coefficient from cell j at frequency i, $\Delta\sigma$ = absorption coefficient difference between frequencies 1 and 2, $\Delta\xi$ = extinction coefficient difference between frequencies 1 and 2 (not including gas being measured) i = 1 or 2 frequencies on or off absorption line, respectively, and j = 1 or 2 for distances R_1 and R_2, respectively. For scattering cells of equal length the resolution length $R_2 - R_1$ equals the scattering cell length Δr. The term $\ln \frac{\beta_{12}\,\beta_{21}}{\beta_{11}\,\beta_{22}}$ is a correction term due to changes in backscattering with frequency across scattering cells. The term $2\int_{R_1}^{R_2}(\Delta\xi)\,dr$ is a correction due to interferent species. Variation in backscatter and interferent absorption at the two frequencies will result in biases in the inferred concentrations. These biases can be reduced by careful frequency selection and partially corrected by using a priori information and auxiliary measurements. For an optically thick species, a series of "on" frequencies is required to maximize sensitivity at various altitudes.

The random error in ρ, which is calculated assuming that signal plus background are measured during each pulse and that background is measured between pulses and subtracted, will depend on the random error in the measurement of P_{ij}. The uncertainty in the inferred concentration $(\delta\rho)^2$ is given by

$$(\delta\rho)^2 = \left(\frac{1}{2\Delta\sigma\Delta r}\right)^2 \frac{1}{N} \sum_{i=1}^{2} \sum_{j=1}^{2} \left[\frac{1}{(SNR)_{ij}^2} + \text{system error terms}\right] \qquad (3)$$

where N is the number of pulse pairs per measurement and SNR is the single pulse signal-to-noise ratio. For heterodyne detection, the major errors in P_{ij} are due to quantum noise in the local oscillator and fluctuation noise in the return signal.

The heterodyne signal-to-noise ratio for a single coherence volume $\frac{P_{ij}}{P_{ij} + BT}$ is limited to 1.0 due to the speckle noise in the return signal. The number of coherence lengths per scattering cell is BT. The number of coherence areas viewed by the detector is M, where M is the ratio of receiver to transmitter area. For heterodyne detection an individual detector is required for each coherence area. The single pulse signal-to-noise ratio for determining the signal from a scattering cell is then

$$SNR = \frac{P_{ij}}{P_{ij} + BT} \sqrt{BTM} \qquad (4)$$

where BTM is the number of statistically independent samples from a scattering cell for a single pulse. The post-detection bandwidth B is constrained by matching with pulse duration ($B \leq 1/T_p$) and by the width of atmospheric spectral lines. The integration time T is constrained by vertical resolution requirements. Neglecting the system error terms, the random error in density for heterodyne detection with bandwidth B, integration time T, N pulse pairs, and M coherence areas with one detector per coherence area is

$$(\delta\rho)^2 = \frac{1}{(2\Delta\sigma\Delta r)^2} \sum_{i=1}^{2} \sum_{j=1}^{2} \left[\frac{P_{ij} + BT}{P_{ij} \sqrt{BTNM}} \right] \tag{5}$$

For N pulse pairs and M detectors, the SNR $\frac{P_{ij}}{P_{ij} + BT} \sqrt{BTNM}$ is maximized for a given total laser energy per measurement ($\propto NMP_{ij}$) when the laser energy per pulse per detector is selected so that $P_{ij} \approx BT$. For that condition an approximate solution to equation (5) is

$$\delta\rho \sim \frac{2}{\Delta\sigma\Delta r} \frac{1}{\sqrt{BTNM}} \propto \frac{1}{\Delta\sigma(\Delta r)^{3/2} \sqrt{BNM}} \tag{6}$$

This equation illustrates that $\delta\rho$ is independent of ρ and proportional to $1/\Delta\sigma$ within the constraint that the two-way integrated absorption through the atmosphere does not limit P_{ij} to less than BT. Equation (6) also indicates the strong effect of range resolution on measurement error. The number of pulse pairs required to maintain a constant measurement error is proportional to the inverse cube of the range resolution.

COMMENTS ON DIRECT DETECTION

Direct detection can have advantages over single-detector heterodyne detection when signal levels are high since direct detection allows averaging over multiple coherence areas with a single detector. The major disadvantage of direct detection is background noise which is limited by optical filters ($\sim 10^{11}$ Hz) compared with the electronic filters (10^6 to 10^9 Hz) for heterodyne detection. Reducing the background noise by reducing the field of view will result in an increase in speckle noise.

The direct detection signal-to-noise ratio can be written as a function of M, the number of coherence areas, and the total direct detected signal $P'_{ij} = MP_{ij}$. The SNR for direct detection (assuming zero detector noise, ref. 3) is

$$(SNR)_{DD} = \frac{P'_{ij} \sqrt{BT}}{\left(P'_{ij} BT + (GDMT)BT + \frac{P'^2_{ij}}{M} \right)^{1/2}} \tag{7}$$

Equation (7) includes a speckle term P'^2_{ij}/M, a Poisson term $P'_{ij}BT$, and a background term $(GDMT)BT$. In equation (7), G is the background signal in detected photons/sec/Hz per coherence area, M is the number of coherence areas, and D is the bandwidth in Hz of the optical filter. Maximization of the direct detection SNR with respect to the number of coherence areas occurs when M is selected so that the background and speckle terms are equal:

$$(SNR)_{DD\ max} \approx \frac{\sqrt{BTM}}{\sqrt{2}} \quad \text{with} \quad M = \frac{P'_{ij}}{\sqrt{GBD}\ T} \tag{8}$$

For this condition, the criterion for direct detection SNR to exceed the single-detector heterodyne large signal SNR of $\sqrt{BT}$ is for $P'_{ij} > 2T\sqrt{GBD}$.

SENSITIVITY ANALYSIS FOR DIAL MEASUREMENT USING HETERODYNE DETECTION WITH A SINGLE DETECTOR

A comprehensive computer algorithm is used to calculate the expectation values of P_{ij} for various measurement conditions. Pressures, temperatures, and gas species densities are input from a midsummer midlatitude atmospheric model. Trace gas species densities can be modified using card inputs. Line absorption parameters are accessed from a comprehensive data base. Sources for line data are given in reference 6. At each altitude, molecular absorption at ν_1 and ν_2 is calculated for each species by summing contributions from absorption lines in the vicinity of the laser frequency. Lorentz, Voigt, or Doppler line shapes are used at appropriate altitudes. Water vapor continuum absorption is added to the line absorption. Extinction due to particulate and molecular scattering is summed with molecular absorption at each altitude to give the total loss in each scattering cell. The integrated two-way loss is calculated by summing contributions from altitude layers between the laser and the cell being considered. The backscattering coefficient β is calculated by combining a Rayleigh term, which is small at infrared frequencies, and a Mie term. Mie backscatter and extinction for the cases shown here are calculated using parameters of Deirmendjian's Haze L size distribution (ref. 7). The vertical aerosol distribution is based on reference 8 with a ground level concentration (350 particles/cm^3) corresponding to a 23-km visibility. Figure 1 shows the Mie contribution to the volume backscatter coefficient used in this study as a function of altitude for $\nu = 927.61\ cm^{-1}$.

For all simulations presented, the overall system efficiency, which is the product of optical and quantum efficiency, is set at 12.5%. The system errors due to amplification and digitization are set at 0.1%. For aircraft and ground-based cases, telescope area is 0.1 m^2 and bandwidth 10^8 Hz; for Shuttle cases, telescope area is 1 m^2 and bandwidth 10^7 Hz. Bandwidths have been constrained by atmospheric line parameters and by laser limits. Pulse energies are selected within practical laser constraints to match signal to bandwidth and the number of pulse pairs N is adjusted to obtain reasonable measurement accuracy. The "on" and "off" frequencies have been selected to be within the range of a single rare isotope multiatmospheric CO_2 laser line. Use of rare isotope lines minimizes interference by atmospheric CO_2 and use of

closely spaced "on" and "off" frequencies minimizes error due to variations in backscatter and interfering species absorption.

Figure 2 displays O_3 concentration in STP-ppb and measurement error in the same units versus altitude for measurement from Shuttle at 250 km. The pulse energy is 5 joules per pulse with 1000 pulse pairs per measurement. Telescope area is 1 m^2, bandwidth is 10^7 Hz, resolution is 1.5 km below 30 km and 3 km above 30 km. Simulations are for an "off" frequency of 1058.01 cm^{-1} and "on" frequencies of 1058.17, 1058.11, and 1058.19 cm^{-1}. It should be noted that a fine tuning of the "on" frequency results in a sharp variation of altitude at which the best measurement can be accomplished.

Figure 3 displays ozone concentration and error in STP-ppb for a measurement from aircraft at 10.5 km looking either upward or downward. Pulse energy is 0.05 joules, telescope area is 0.1 m^2, bandwidth is 10^8 Hz, and "on" frequency is 1058.20 cm^{-1}. In the case of aircraft measurements the "on" frequency selection is simplified since the signal does not have to pass through the ozone bulge. Two cases are presented in order to illustrate the strong influence of range resolution on number of pulses required for a measurement. The solid error line is for 3000 pulse pairs with a resolution of 0.5 km below 6 km, 1 km from 6 to 10 km, and 3 km above 10 km. The dashed error line is for 100 pulse pairs with a resolution of 1.5 km. The errors are nearly identical at low altitude, which is expected (see equation (6)) since the number of pulses has been increased by approximately the cube of the inverse of the range resolution.

Figure 4 displays NH_3 concentration and error in STP-ppb for 300 pulse pairs with operation from Shuttle at an altitude of 250 km with 1 joule per pulse and from aircraft at an altitude of 10 km with 0.05 joules per pulse. Since NH_3 is not heavily attenuated, only one set of frequencies is required. The resolution for both cases is 1.5 km.

Figure 5 displays NH_3 concentration and error in STP-ppb for a ground-based measurement. The vertical NH_3 distribution is the same as shown in figure 4. For this case, the telescope area is 0.1 m^2, bandwidth is 10^8 Hz, "on" frequency is 927.32 cm^{-1}, and "off" frequency is 927.61 cm^{-1}. The error curves are for a range resolution of 1.5 km using 300 pulse pairs. The two error curves are for laser energies of 0.05 J and 0.5 J. Note that for the cases in which E = 0.5 J, the large signal limit $\left(\frac{P_{ij}}{P_{ij} + BT} \approx 1\right)$ is achieved throughout the entire measurement range and therefore the error is nearly independent of altitude.

Figure 6 is for the same conditions as shown in figure 5 with the exception that the NH_3 concentration has been reduced by a factor of 5. The error is plotted only for the E = 0.05 J case. Comparison of figure 6 with the 0.05 joule curve in figure 5 illustrates the effect of concentration on measurement error. At low altitude, $P_{ij} \geq BT$ and the measurement errors are independent of concentration. At higher altitudes $P_{ij} < BT$ and the increased integrated absorption at the higher concentration (fig. 5) results in an increased measurement error for that case. These NH_3 distributions are

typical values from Langley Research Center ground-based infrared heterodyne radiometer measurements (ref. 9).

Figure 7 displays percent error in measurement of water vapor concentration versus altitude for measurement from 250 km for a midsummer, midlatitude water vapor distribution. Measurement conditions are 1 joule per pulse, 100 pulse pairs, 10^7 Hz bandwidth, and 1 m^2 telescope. Two "on" frequencies are used at 948.25 and 948.30 cm^{-1}. The "off" frequency is at 948.35 cm^{-1}. Tropospheric water vapor is particularly amenable to measurement from space since the concentration rapidly increases towards the ground. Thus, absorption is high at low altitudes and the integrated absorption from space to low altitudes is relatively low. For measurement of water vapor at higher altitudes, the number of pulses would have to be increased.

CONCLUDING REMARKS

High vertical resolution measurement of atmospheric trace species can be achieved using CO_2 laser DIAL with heterodyne detection. This study indicates that maximum sensitivity at minimum laser energy per measurement requires multiple pulse operation with the energy per pulse selected so that the measure photon rate is approximately equal to the detector IF bandwidth. Measurement sensitivities can be maximized and interference effects minimized by fine adjustment of measurement frequencies using the tunability of high-pressure laser The use of rare isotope lasers minimizes loss due to CO_2 atmospheric absorption

REFERENCES

1. Shuttle Atmospheric Lidar Research Program - Final Report of Atmospheric Lidar Working Group. NASA SP-433, 1979.

2. Jakeman, E.; Oliver, C. J.; and Pike, E. R.: Optical Homodyne Detection Advances in Physics. Europhysics Journal, vol. 24, no. 3, May 1975.

3. Elbaum, M.; and Teich, M. C.: Heterodyne Detection of Random Gaussian Signals in the Optical and Infrared: Optimization of Pulse Duration. Optics Communications, vol. 27, Nov. 1978.

4. Rye, B. J.: Differential Absorption Lidar System Sensitivity With Heterodyne Reception. Appl. Optics, vol. 17, no. 24, Dec. 15, 1978.

5. Remsberg, E. E.; and Gordley, L. L.: Analysis of Differential Abosrption Lidar From the Space Shuttle. Appl. Optics, vol. 17, no. 4, Feb. 15, 1978.

6. Park, J. H.: Optical Measurement in the Middle Atmosphere. Pageoph, vol. 117 (1978/79).

7. Deirmendjian, D.: Electromagnetic Scattering on Spherical Polydispersions. American Elsevier Publishing Co., New York, NY, 1969.

8. McClatchey, Robert A.; and Selby, John E. A.: Atmospheric Attenuation of Laser Radiation From 0.76 to 31.25 μm. AFCRL-TR-74-0003, U.S. Air Force, Jan. 1974.

9. Hoell, J. M.; Harward, C. M.; and Williams, B. S.: Remote Infrared Heterodyne Radiometer Measurements of Atmospheric Ammonia Profiles. Geophys. Res. Lett., Vol. 7, No.5, May 1980, pp. 313-316.

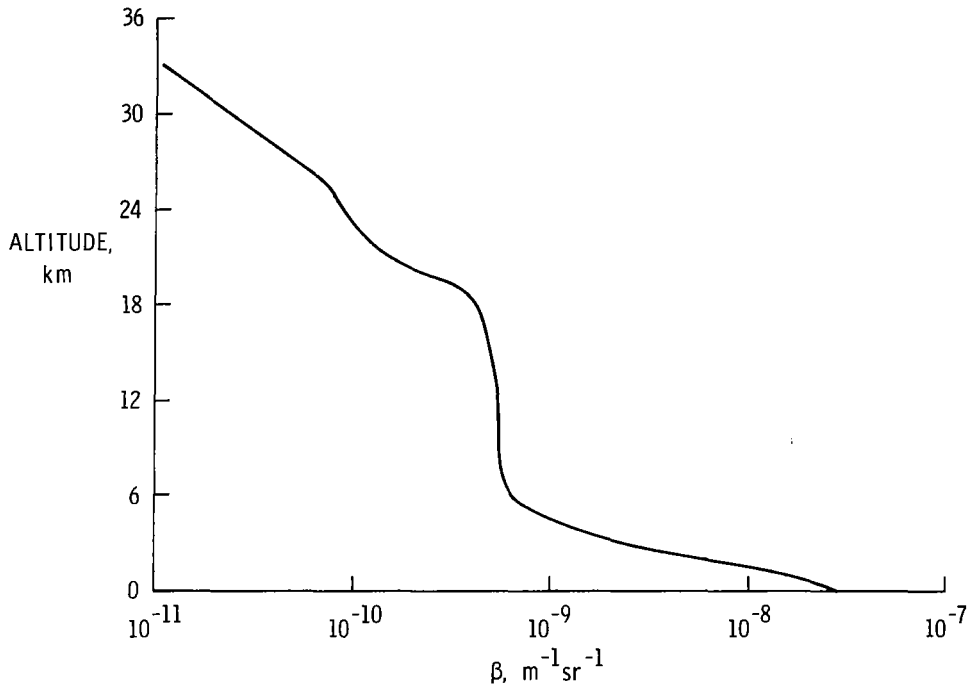

Figure 1.- Aerosol volume backscattering coefficient as a function of altitude for ν = 927.61 cm^{-1}.

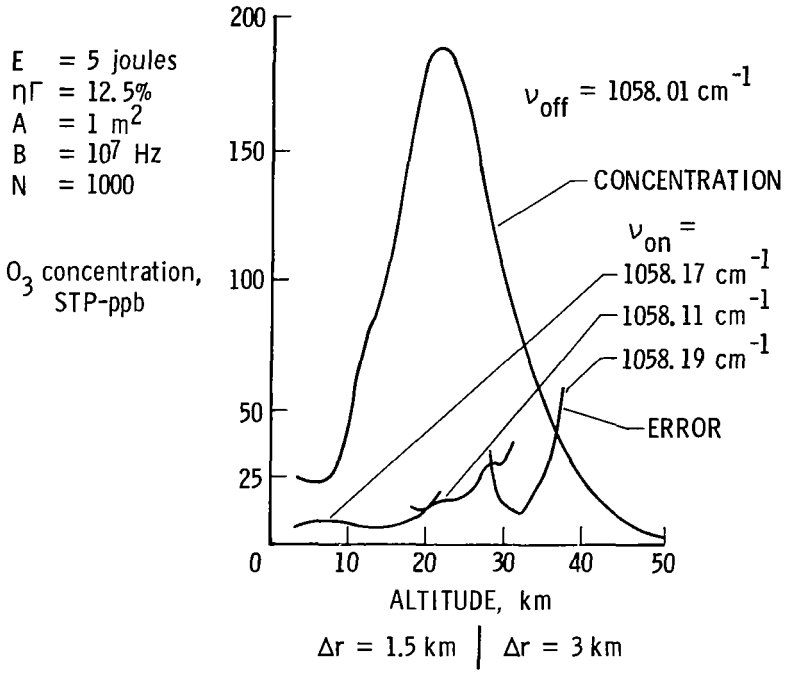

Figure 2.- Ozone measurement from 250 km.

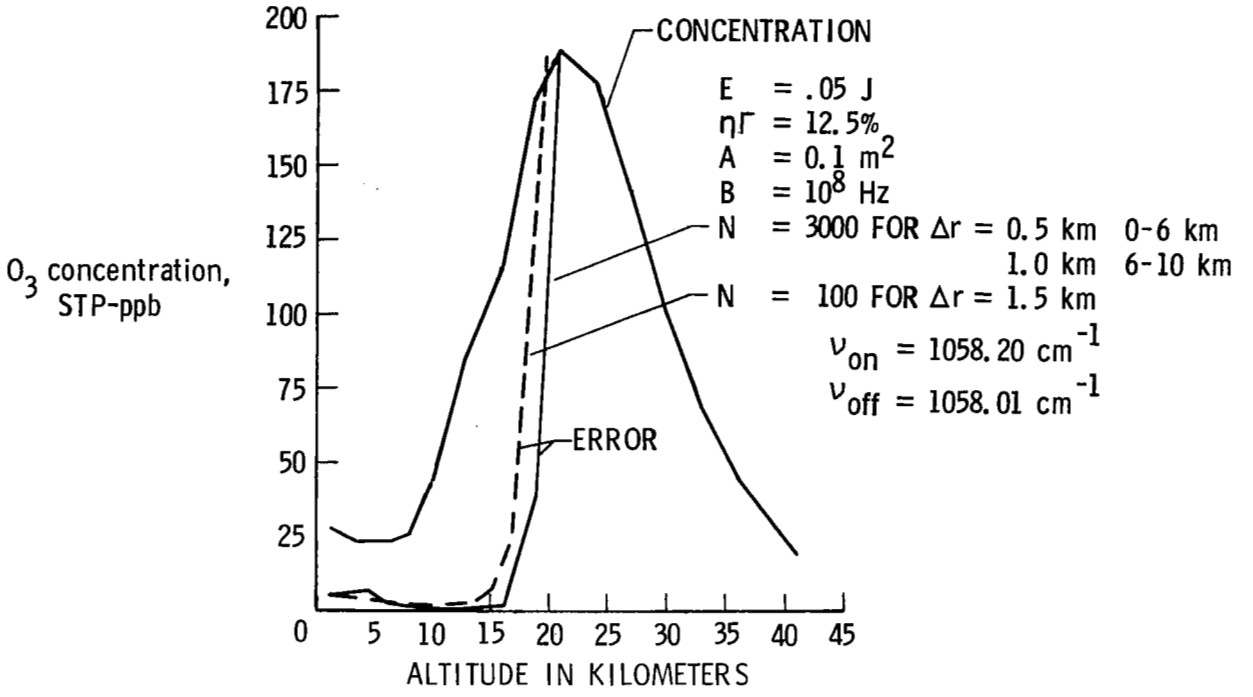

Figure 3.- Ozone measurement from 10.5 km.

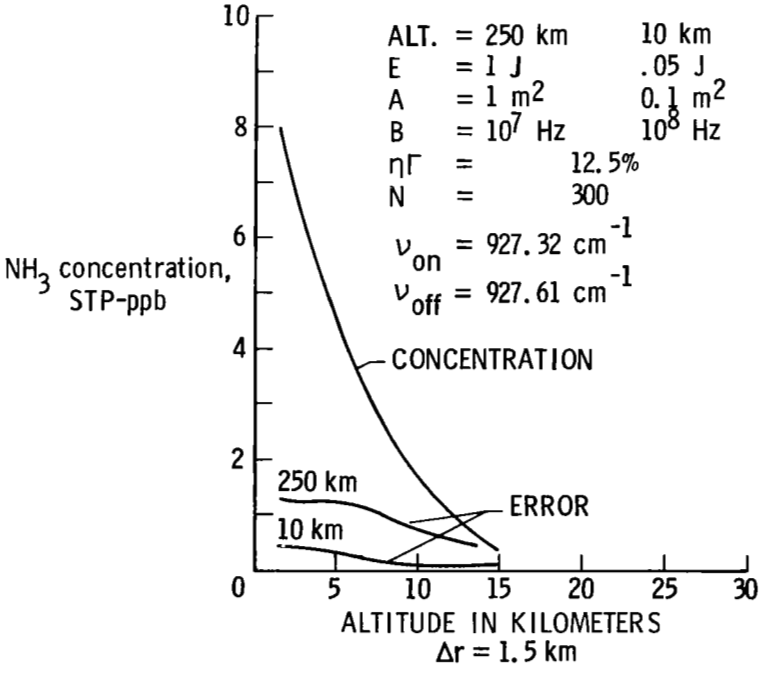

Figure 4.- NH_3 measurement from 10 and 250 km.

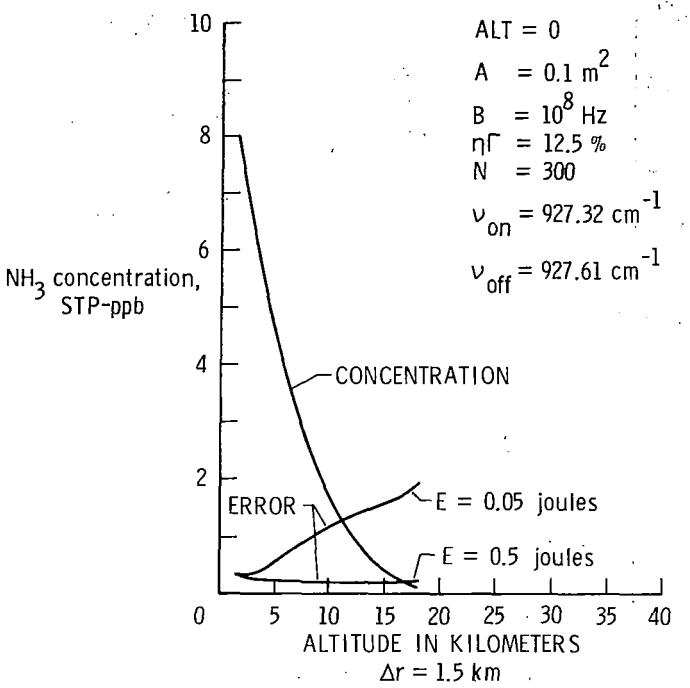

Figure 5.- NH_3 measurement from ground for E = 0.5 and 0.05 J.

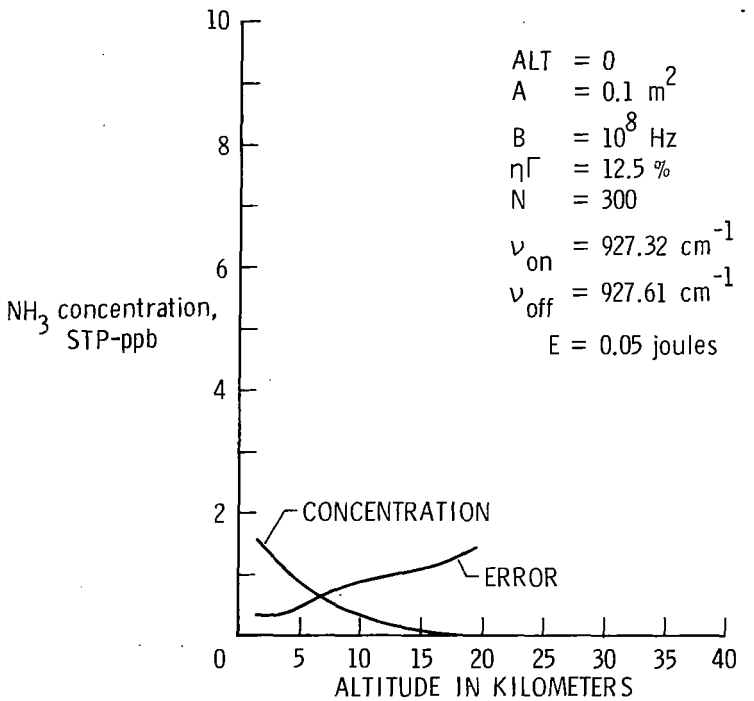

Figure 6.- NH_3 measurement from ground for E = 0.05 J.

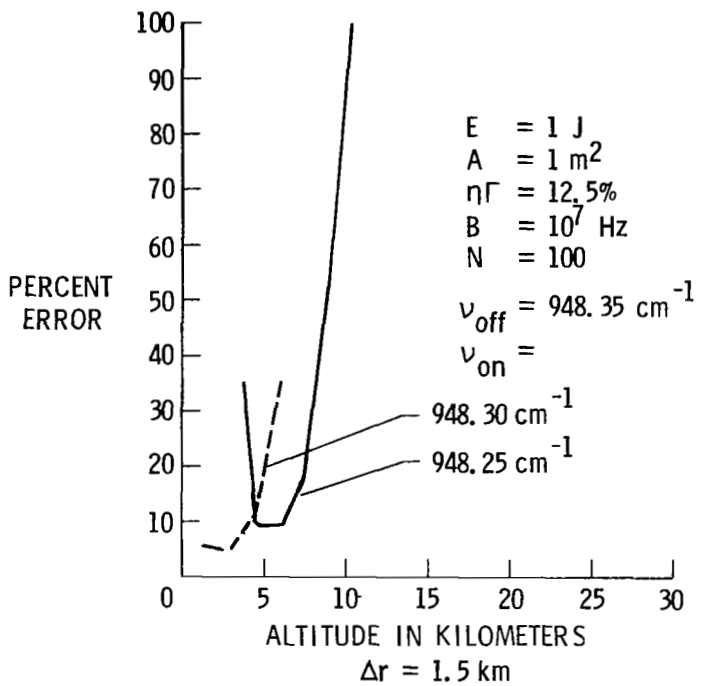

Figure 7.- Water vapor measurement from 250 km.